International Journal of Theoretical Physics, Vol. 31, No. 8, 1992

Characterization of Chaos

Daniel M. Heffernan,[1,2] P. Jenkins,[1] M. Daly,[1] B. J. Hawdon,[1,3] and J. O'Gorman[1,4]

Received December 6, 1991

We give a brief introduction to chaos and its characterization. We examine some standard systems in detail from the perspective of chaos and review their properties. Concepts necessary to understand them, such as dimension, are also reviewed. To illustrate the main ideas, we choose three examples which have served as paradigms for the study of chaos in physical systems, namely, the Hénon discrete mapping, the Lorenz system of coupled ordinary differential equations, and the Mackey–Glass infinite-dimensional delay differential equation.

1. INTRODUCTION

In recent years a field of study has developed which we now call *chaos.* This paper is an introduction to this field of study. It is a review article which is designed to acquaint scientists and engineers with recent developments in the area of the *characterization of chaos.* No attempt is made to assemble a complete bibliography, as the review is pedagogically motivated and reflects the authors' view of the recent history of the field. We restrict our discussion to chaos and its characterization and mention very little about the routes to chaos, as these are extensively reviewed elsewhere (Cvitanovic, 1989; Hao Bai-lin, 1984). A more complete introduction to the whole area is provided by the reprint collections of Cvitanovic (1989), Hao Bai-Lin (1984), the books of Schuster (1988) and Bergé *et al.* (1987), and the review article of Eckmann and Ruelle (1985).

[1]School of Physical Sciences, Dublin City University, Dublin 9, Ireland.
[2]Also with the School of Theoretical Physics, Dublin Institute of Advanced Studies, Dublin 4, Ireland.
[3]Permanent Address: 4 Physikalisches Institut, University of Stuttgart, Stuttgart, Germany.
[4]Permanent Address: AT&T Bell Laboratories, Murray Hill, New Jersey.

0020-7748/92/0800-1345$06.50/0

2. SENSITIVE DEPENDENCE ON INITIAL CONDITIONS

We will limit our discussion to differentiable dynamical systems defined by the equation

$$\frac{dx}{dt} = F(x) \qquad \text{(continuous time } t\text{)}$$

or by the map

$$x_{n+1} = f(x_n) \qquad \text{(discrete time)}$$

where $x(t)$ is a vector in finite- or infinite-dimensional space and F and f are differentiable autonomous (i.e., have no explicit time dependence) functions.

We have a sensitive dependence on initial conditions if for a small change $\delta x(0)$ in the initial conditions there is an exponential growth in the separation of the points, i.e.,

$$|\delta x(t)| \approx |\delta x(0)| e^{\lambda t} \tag{1}$$

where $\lambda > 0$. "Chaos is the prevalence of sensitive dependence on initial conditions, whatever the initial condition is" (Ruelle, 1990). As pointed out by Ruelle (1990), it was Hadamard (1898) who first observed this sensitive dependence on initial conditions in a special system and Duhem (1906) and Poincaré (1908) who first realized that for a system such as that studied by Hadamard one could not make long-term predictions. Mathematicians, after a considerable lapse of time, following the ideas of Hadamard have now proved the existence of chaos in a number of systems (Smale, 1967; Ruelle, 1990). However, it has been the advent of computers and the work of Lorenz (1963), Feigenbaum (1978, 1979), Ruelle and Takens (1971), and others (Cvitanovic, 1989; Hao Bai-lin, 1984) which has revolutionized the whole area of nonlinear dynamics and brought the new science of chaos to a wide audience.

3. STRANGE ATTRACTORS

In what follows we will restrict our discussion to dissipative dynamical systems. There are a number of attractors possible in such systems, for example, fixed points, limit cycles, two tori, and strange attractors. A *strange attractor* is an attractor with sensitivity to initial conditions. Strange attractors are in general low-dimensional. They may or may not be self-similar and have a noninteger dimension. We examine some standard systems in detail from the perspective of chaos and review their properties. Concepts necessary to understand them, such as dimension, are also reviewed. To

illustrate the main ideas, we choose three systems which have served as paradigms for the study of chaos in physical systems, namely the Hénon discrete mapping, the Lorenz system of coupled ordinary differential equations, and the Mackey–Glass infinite-dimensional delay differential equation. These systems are interesting in themselves and are not yet fully understood. By their study we hope to illustrate some of the exciting quantitative science that has evolved over the last 20 years and which has contributed so much to our understanding of chaos and given us a fundamentally new perspective on the whole area of nonlinear dynamics.

4. HÉNON MAP

In this section we will examine the dynamical behavior of the well-known quadratic, two-dimensional invertible map introduced by Hénon (1976):

$$\begin{aligned} X_{i+1} &= 1 + Y_i - aX_i^2 \\ Y_{i+1} &= bX_i \end{aligned} \tag{2}$$

where a and b are constants, $a > 0$ and $0 < b < 1$. Starting with an initial point (X_0, Y_0), we calculate (X_1, Y_1) and the succeeding points by iteration. The two fixed points $(X_\pm^*, Y_\pm^*)$ are obtained by setting $X_{i+1} = X_i$ and $Y_{i+1} = Y_i$ and are given by

$$(X_\pm^*, Y_\pm^*) = \left(\frac{(b-1) \pm [(b^2-1)+4a]^{1/2}}{2a}, bX_\pm^* \right)$$

In the following we fix $b = 0.3$ and investigate the stability of the fixed points as the parameter a is varied. The stability is determined from the eigenvalues given by

$$\lambda_\pm = -aX_\pm^* \pm [a^2 X_\pm^{*2} + b]^{1/2} \tag{3}$$

The fixed point (X_-, Y_-) is always unstable, whereas (X_+, Y_+) undergoes a flip bifurcation ($\lambda = 1$) when $a_1 > 3/4(1-b)^2 = 0.3675$. At a_1 both fixed points are unstable; hence there is a bifurcation from an attractor of period 1 to an attractor of period 2. As a is increased, successive bifurcations occur, until there is an infinite periodic attractor at a_∞. This is clearly represented in the bifurcation diagram of Figure 1 for the parameter range $0.85 < a < 1.40$, where period-two and subsequent bifurcations are shown.

As a approaches a_∞ the sequence of bifurcations a_n gets rapidly narrower. Feigenbaum (1978), using the renormalization group techniques developed by K. Wilson (Wilson and Kogut, 1974), analyzed similar sequences at which period doubling occurs and found that the convergence rate

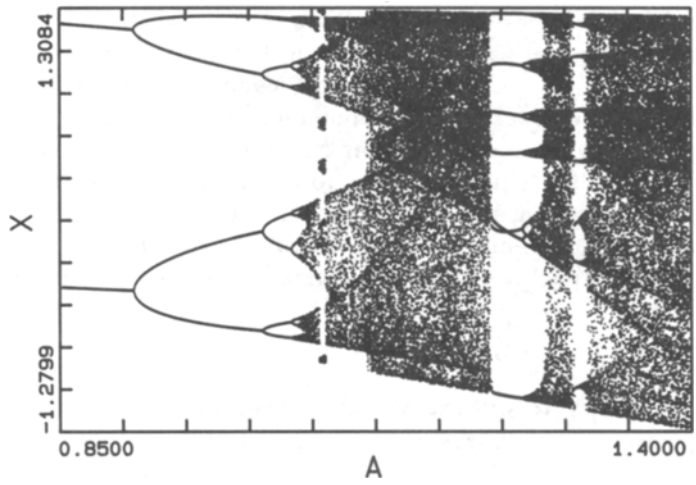

Fig. 1. Bifurcation diagram of the Hénon map in the parameter range $b = 0.3$ and $0.85 < a < 1.40$.

is given by

$$\delta = \lim_{n \to \infty} \frac{a_n - a_{n-1}}{a_{n+1} - a_n} = 4.6692016$$

Feigenbaum's constant δ is universal for all maps with quadratic maxima.

Of particular interest is the behavior of this system for $a > a_\infty$ ($\cong 1.0580\ldots$). The parameter chosen by Hénon was $a = 1.4$. For this parameter we have generated a sequence of points from the mapping equation (2). A plot of its phase space (X_i vs. Y_i) is shown in Figure 2a. As time evolves, the sequence of data X_i, Y_i fall randomly on this chaotic attractor. As yet there is no rigorous mathematical proof that this is a strange attractor despite the extreme simplicity of the two-dimensional mapping. Figure 2b is a magnified view of the small square in Figure 2a and the enlargement shows that each of these lines is in fact composed of more than one line. Successive enlargements in Figures 2c and 2d reveal more line structure. These figures strongly suggest that structure is present at all scales of resolution.

The Jacobian of the Hénon map given by equation (1) is

$$J(X_n, Y_n) = \begin{vmatrix} \delta X_{n+1}/\delta X_n & \delta X_{n+1}/\delta Y_n \\ \delta Y_{n+1}/\delta X_n & \delta Y_{n+1}/\delta Y_n \end{vmatrix} = \begin{vmatrix} -2aX_n & 1 \\ b & 0 \end{vmatrix} = -b$$

For $b < 1$ the map is area-contracting, i.e., the modulus of the Jacobian determinant is less than unity. Each iteration multiplies the area by a factor

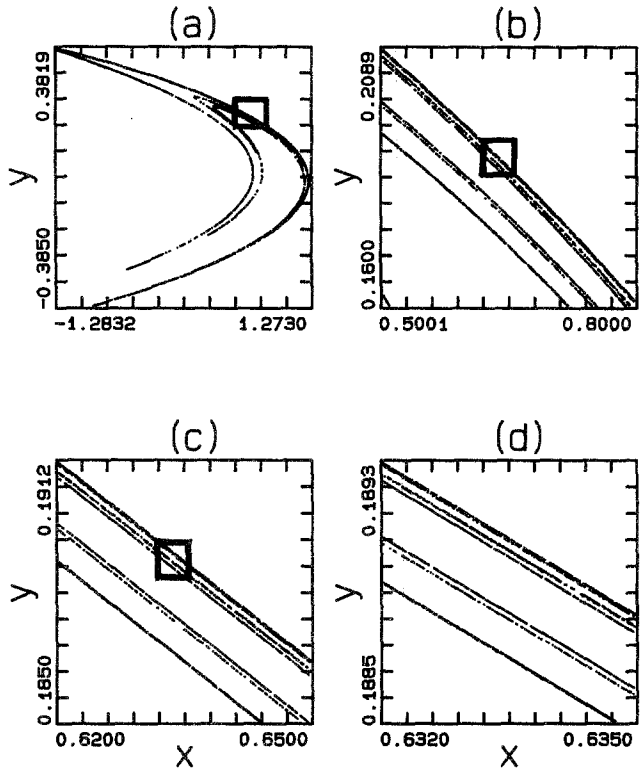

Fig. 2. Self-similarity in the Hénon attractor. (a) Hénon attractor at $a = 1.4$, $b = 0.3$. (b-d) Successive enlargements of the square in (a).

b. Hence all the attractors of this system, including the strange attractor in Figure 2a, have a contracting phase space area.

5. THE STRANGE ATTRACTOR OF LORENZ

Lorenz (1963) observed chaotic behavior in a system of three first-order ordinary differential equation. These quadratic, nonlinear differential equations have the form

$$\begin{aligned} \frac{dX(t)}{dt} &= -\sigma(X - Y) \\ \frac{dY(t)}{dt} &= -Y - XZ + rX \\ \frac{dZ(t)}{dt} &= XY - bZ \end{aligned} \tag{4}$$

Lorenz obtained this system of equations from a Fourier modal decomposition of a set of partial differential equations describing a viscous, thermal conducting fluid heated from below (Rayleigh-Bénard problem). σ, r, and b are constants greater than zero. Haken (1978) showed that the same equations describe a single-mode homogeneously broadened laser. In order to examine the time evolution of the variables $X(t)$, $Y(t)$, and $Z(t)$, it is necessary to integrate the coupled equations (4) numerically by routine computer algorithms since these equations cannot be solved analytically.

The fixed points are obtained by setting the derivatives equal to zero:

$$\begin{aligned} &X^* = Y^* = Z^* = 0 \\ &X^* = Y^* = [b(r-1)]^{1/2}, \qquad Z^* = r-1 \\ &X^* = Y^* = -[b(r-1)]^{1/2}, \qquad Z^* = r-1 \end{aligned} \tag{5}$$

The stability of these fixed points is determined by linearizing the right-hand side of equation (4) and finding the eigenvalues λ of

$$\det\begin{pmatrix} -\sigma-\lambda & \sigma & 0 \\ r-Z^* & -1-\lambda & -X^* \\ Y^* & X^* & -b-\lambda \end{pmatrix} \tag{6}$$

For the fixed point $(0, 0, 0)$ the eigenvalues of this 3×3 matrix are

$$\begin{aligned} \lambda_1 &= -b \\ \lambda_{2,3} &= -\tfrac{1}{2}(\sigma+1) \pm \tfrac{1}{2}[(\sigma-1)^2 - 4\sigma r]^{1/2} \end{aligned} \tag{7}$$

When $r<1$ there is only one fixed point, the origin, and its eigenvalue is negative, hence the origin is an stable attractor. When $r>1$ the origin is no longer attracting, but we have two additional fixed points and their stability is determined from the following conditions:

$$\sigma > b+1 \qquad \text{and} \qquad r \geq \sigma(\sigma+b+3)/(\sigma-b-1) \tag{8}$$

Choosing $\sigma = 3$ and $b = 1$, we find that the two fixed points are no longer attracting for $r \geq 21$. If we numerically integrate the Lorenz equations with $r = 5$, the origin is unstable but the other two fixed points are stable and the solution converges onto one of these simple fixed-point attractors as shown in Figure 3a. The corresponding phase plot in Figure 3b, is a point after initial transients have decayed. Which of the two fixed points it converges to depends on the initial condition used to obtain the solution of the Lorenz equation. At $r = 21$ all three fixed points are unstable. A Hopf bifurcation occurs, i.e., the imaginary part of the eigenvalue takes on a positive real part.

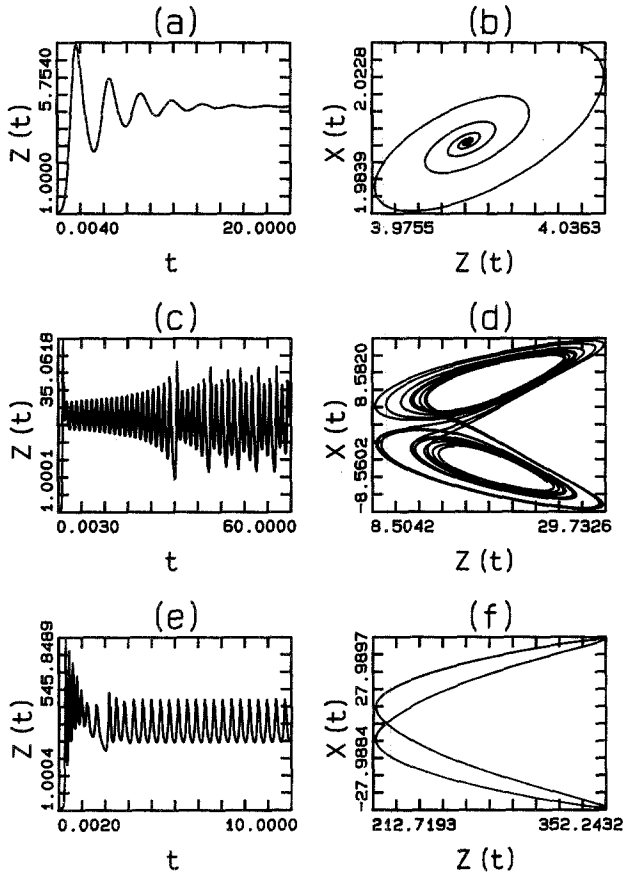

Fig. 3. Graphical solutions for the Lorenz system of equation (4). Left-hand side: the time evolution $Z(t)$ vs. t; right-hand side: $X(t)$ vs. $Z(t)$, for $\sigma = 3$, $b = 1$, and (a, b) $r = 5.0$; (c, d) $r = 21.0$; (e, f) $r = 280.0$

When all fixed points of a system are unstable we can get chaotic behavior. As an example we have integrated the Lorenz equations for $r = 21$. The time evolution [$Z(t)$ vs. t] and a phase space plot [$X(t)$ vs. $Z(t)$] for $r = 21$ are shown in Figures 3c and 3d, respectively. As the phase space plot evolves with time, the trajectory $Z(t)$ appears to switch from the neighborhood of one of the (unstable) fixed points to the other in an apparently random fashion.

For very large r, nearly all trajectories are attracted to stable limit cycles. An example of one of these limit cycles is shown in Figure 3f for $r = 280$. Once initial transients have decayed, the time evolution of $Z(t)$ in Figure 3e is periodic.

Figure 4 shows the power spectrum of the Lorenz strange attractor at $r = 21$. The power spectrum was obtained with a FFT algorithm after initial transients have decayed away. We see the characteristic broadband spectrum of chaos. This type of spectrum is typical of chaotic systems.

An informative illustration of the sensitive dependence on initial conditions for the Lorenz system is shown in Figure 5 (Crutchfield *et al.*, 1986). Lorenz equations are numerically integrated 1000 times with 1000 slightly different initial conditions (i.e., seed values). These 1000 initial measurements are represented by a dot in Figure 5a, initially so close that they are indistinguishable. As each point moves under the action of equation (4) the indistinguishable points at time $t = 0$ have spread over the entire attractor at $t = 60$ as shown in Figure 5d. Prediction has now become impossible, the final state can be anywhere on the attractor. Such a degree of sensitivity on initial conditions is never exhibited for regular periodic systems. This exponential divergence of nearby trajectories (or initial measurements) is the underlying reason why chaos leads to unpredictability.

Using the Lie derivative, we can calculate the contraction of the volume in phase space of the Lorenz system given by equation (4), i.e.,

$$\frac{\delta \dot{X}}{\delta X} + \frac{\delta \dot{Y}}{\delta Y} + \frac{\delta \dot{Z}}{\delta Z} = -(r + b + 1) = -5$$

This system is highly dissipative with a contraction rate of $\exp(-5)$. As phase space evolves in time according to equation (4), the enclosed volume contracts exponentially.

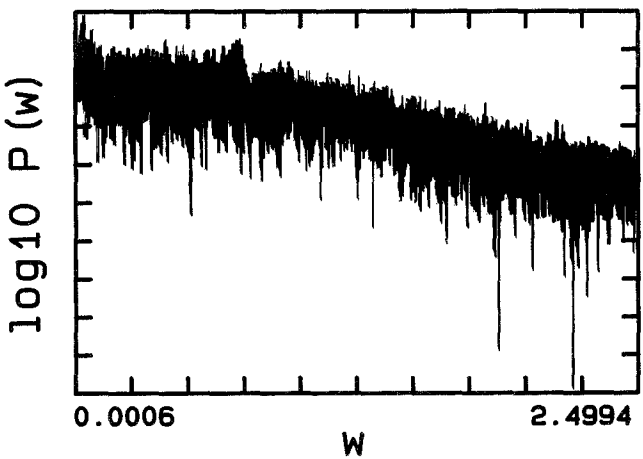

Fig. 4. Power spectrum for the Lorenz strange attractor at $r = 21$. This spectrum is obtained from the average of 80 individual FFTs each of sample length 8192 taken at intervals $\Delta t = 0.2$.

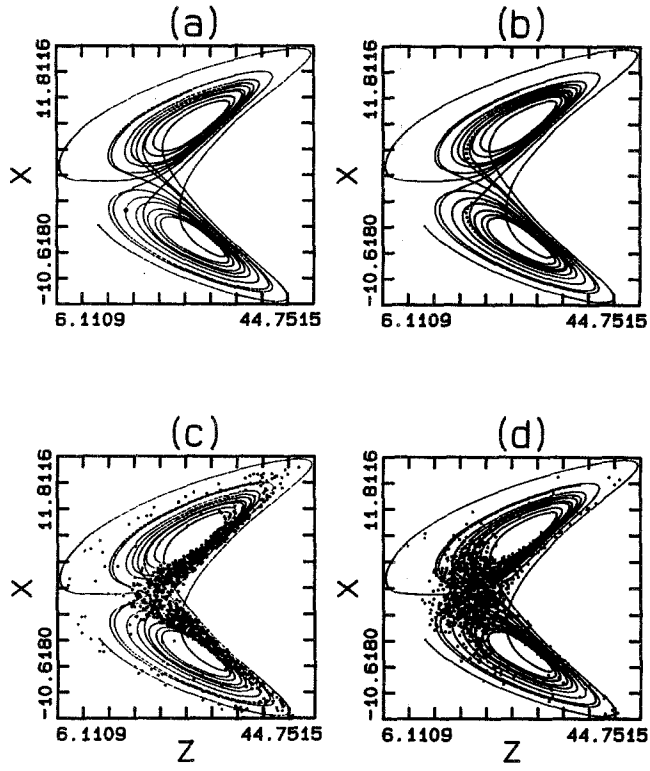

Fig. 5. An illustration of the divergence of initial measurements. Time evolution of the initial conditions at different times t: (a) 0, (b) 20, (c) 40, and (d) 60. For reference the Lorenz attractor is shown in the background.

6. DELAY DIFFERENTIAL EQUATIONS

Delay differential equations provide an exciting testing ground for many of the mathematically untested conjectures of chaos and its characterization. In this section we will examine the dynamical behavior of an infinite-dimensional system which consists of a first-order nonlinear differential equation with a time delay:

$$\frac{dX(t)}{dt} = f(X(t), X(t-\tau))$$

Nonlinear time delay equations have been used to describe optical systems that exhibit bistability (Hopf *et al.* 1986; Vallée *et al.*, 1986) and to model isolated populations (de Oliveira and Malta, 1987). A very thorough investigation has been carried out by Farmer (1982) on the following nonlinear

delay equation:

$$\frac{dX(t)}{dt} = \frac{aX(t-\tau)}{1+X(t-\tau)^c} - bX(t)$$

This equation is due to Mackey and Glass (1977) and is a model for blood production in patients with leukemia. To calculate $X(t)$ numerically for a time greater than t, a function $X(t)$ over the interval $(t, t-\tau)$ must be given. Thus, equations of this type are infinite-dimensional and can display chaotic behavior since their topological phase space dimension is greater than three, the minimum dimension required, since chaos in two-dimensional continuous systems is forbidden by the Poincaré-Bendixson theorem (Hirsch and Smale, 1965). For the parameters a, b, and c equal to 0.1, 0.2, and 10, respectively, chaotic solutions are observed as the delay parameter τ is varied.

The fixed point X^* of the system is obtained by setting $dX/dt = 0$ and $X^* = X(t) = X(t-\tau)$. A linear stability analysis shows that this fixed point is stable for $\tau < 4.53$. The solution becomes unstable via a Hopf bifurcation as τ is increased (Marsden and McCracken, 1976). For $4.53 < \tau < 13.3$ numerical simulation shows that there is a stable limit cycle attractor. At $\tau = 13.3$ the period of this limit cycle doubles, initiating a period-doubling bifurcation sequence which accumulates at $\tau = 16.8$. De Oliveria and Malta (1987) have verified that the rate of bifurcation is close to the universal Feigenbaum value of $\delta = 4.6692\ldots$.

For $\tau > 16.8$ numerical solutions show chaotic attractors interspersed with windows of periodic behavior where stable limit cycles are found. Figures 6a and 6b show chaotic attractors for two parameter values $\tau = 19.8$

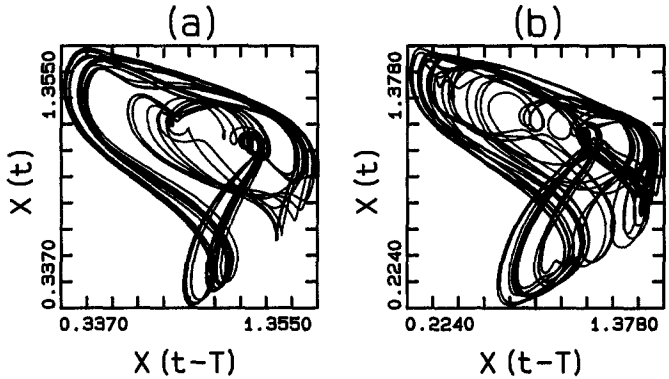

Fig. 6. Phase space evolution with $a = 0.2$, $b = 0.1$, $c = 10$, and (a) $\tau = 19.8$ and (b) $\tau = 30$, where τ is the delay parameter.

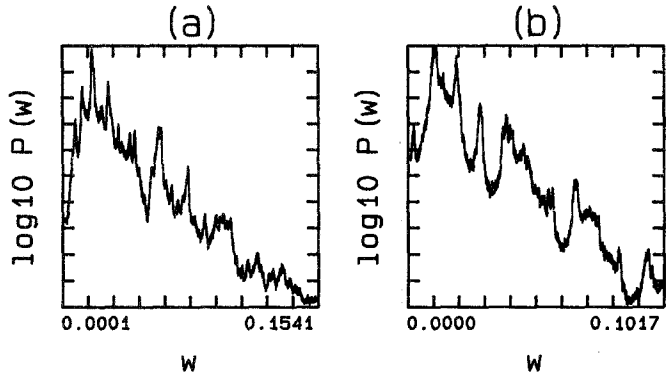

Fig. 7. Power spectra corresponding to Figure 6. Each spectrum was obtained from the average of 100 individual FFTs each of sample length 8192 taken at intervals $\Delta t = 3.0$. These plots are on a semilog scale.

and 30.0, and Figure 7a and 7b show their corresponding broadband power spectra. A broadband power spectrum is characteristic of chaos and shows the sensitive dependence on initial conditions. The phase space plot at $\tau = 30$ is considerably more complicated and the power spectrum contains less pronounced peaks.

Information about the structure of these chaotic attractors can be obtained by using the Poincaré map (or surface of section) technique. This entails plotting $X(t-\tau)$ against $X(t-2\tau)$ whenever $X(t) = \text{const}$, which is arbitrary, and in this case we take it to be 1.05. Shown in Figure 8a is a cross section of the chaotic attractor for $\tau = 19.8$. The structure within structure is clearly apparent in the enlargement, Figure 8b. In contrast to

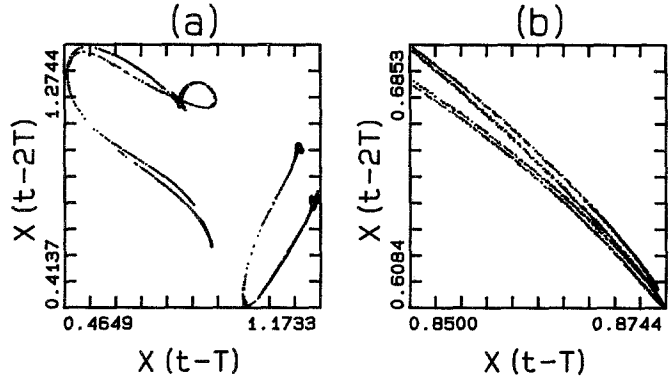

Fig. 8. (a) A cross section of the chaotic attractor for $\tau = 19.8$ and (b) an enlargement showing structure within structure.

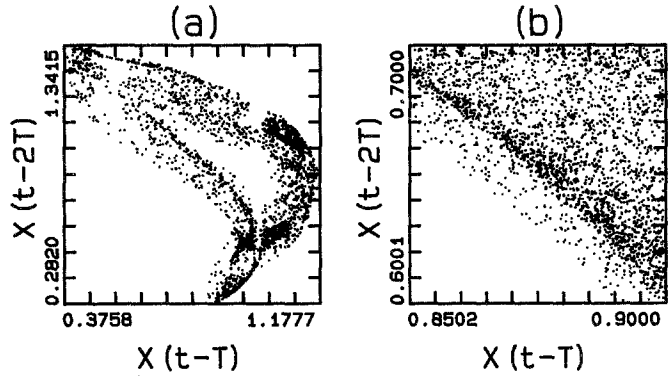

Fig. 9. (a) A cross section of the chaotic attractor for $\tau = 30$ and (b) an enlargement which does not show structure.

this, the surface of section at $\tau = 30.0$, Figures 9a and 9b, does not show the same self-similarity that was present at $\tau = 19.8$. The attractor has a far more complicated appearance.

Each of the chaotic attractors introduced by the previous examples is dissipative and therefore has a contracting phase space area. However, this does not mean that their dimension is zero; as will be shown in the next section, the dimension of the these chaotic attractors is noninteger and less than the phase space dimension.

7. THE CONCEPT OF DIMENSION

In this section we give a brief introduction to the characterization of chaotic dynamical systems in terms of dimensions. In particular, we examine the Lyapunov characteristic exponents (LCE), the generalized dimension spectrum, the $f(\alpha)$ spectrum, and the relationship between them.

We now elaborate on the meaning of equation (1) by considering a one-dimensional map of the form

$$X_{n+1} = f(X_n)$$

The LCE can be obtained as follows. The initial point X_0 and the point $X_0 + \varepsilon$ will after N iterations be separated by the amount (Schuster, 1988)

$$\varepsilon\, e^{N\lambda(X_0)} = |f^N(X_0 + \varepsilon) - f^N(X_0)|$$

which in the limit $\varepsilon \to 0$ and $N \to \infty$ gives the LCE for a one-dimensional map:

$$\lambda(X_0) = \lim_{N\to\infty} \frac{1}{N} \ln \left| \frac{df^N(X_0)}{dX_0} \right| = \lim_{N\to\infty} \frac{1}{N} \sum_{i=0}^{N-1} \ln |f'(X_i)|$$

where $f' = df/dX$. The LCE measures the exponential separation of nearby

points (see Figure 10). It is effectively a measure of the average loss of information about the position of the point. The definition can be generalized to multidimensional mappings and continuous systems (Schuster, 1988, and references therein).

The spectrum of LCE has proven to be one of the most useful dynamical tools for the examination of chaotic systems. The LCE measure the average exponential divergence of nearby trajectories when they are positive and the average convergence rate when they are negative. There is one characteristic exponent for each phase space dimension of the dynamical system. The spectrum of LCE provides a useful means of classifying attractors. For example, a three-dimensional system of ordinary differential equations with all negative exponents is a fixed point and the LCE spectrum is denoted by $(-,-,-)$. A spectrum $(0,-,-)$ indicates that the attractor is a limit cycle. Thus, $(+,0,-)$, for example, would indicate a chaotic attractor in three-dimensional phase space. A positive exponent is a necessary condition for chaos. In Table I we list the LCE spectra for each of the three systems we have examined above.

Numerical evidence supports the following conjecture by Kaplan and Yorke (1979) for relating the LCE spectra to the fractal dimension:

$$D_{\mathrm{L}} = j + \frac{\sum_{i=1}^{j} \lambda_i}{|\lambda_{j+1}|}$$

where it has been assumed the Lyapunov exponents are ordered, $\lambda_1 > \cdots > \lambda_N$, and j is the largest integer so that $\lambda_1 + \cdots + \lambda_j \geq 0$. The quantity D_{L} is referred to as the Lyapunov dimension. Based on the above conjecture a fixed point has dimension zero and a limit cycle has dimension one. Chaotic attractors usually have noninteger dimensions, as is apparent from the D_{L} values listed in Table I for the Hénon, Lorenz, and Mackey-Glass systems. The LCE spectrum for the Mackey-Glass system consists of an infinite number of Lyaponov exponents of which the most positive are listed in Table I. The Lyaponov dimension D_{L} of the Mackey-Glass chaotic attractors at delay parameter $\tau = 19.8$ and $\tau = 30$ is 2.27 and 3.58, respectively. Farmer (1982) has shown that the dimension increases monotonically within τ and for $\tau = 350$ the dimension is of the order of 20.

Most definitions of dimension use the notion of partitioning phase space into boxes of size l. Suppose that there is an attractor in phase space

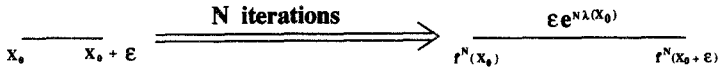

Fig. 10. The separation of neighboring points X_0 and $X_0+\varepsilon$ after N iterations is $f^N(X_0+\varepsilon)-f^N(X_0)$.

Table I. Estimates of the LCE Spectrum, the Lyaponov Dimension D_L, and the Correlation Dimension D_2 for the Hénon, Lorenz, and Mackey-Glass Systems

Attractor Type	LCE spectra	D_L	D_2
Henon Map:			
Fixed point $a < a_\infty$	$(-, -)$	0.0	0.0
Chaotic $a = 1.40$	$(.42, -1.62)$	1.26	1.24
Lorenz:			
Fixed point $r = 5.0$	$(-.29, -.29, -4.41)$	0.0	0.0
Limit cycle $r = 280$	$(0, -2.49, -2.51)$	1.0	1.0
Chaotic $r = 21$	$(0.41, 0, -5.41)$	2.08	2.06
Mackey Glass:			
Chaotic $\tau = 19.8$	$(.0077, 0, -.029, -0.39, ..)$	2.27	2.21
Chaotic $\tau = 30.0$	$(.0069, .0023, 0, -.015, -.024, ..)$	3.58	3.11

and the trajectory $X(t)$ is in the basin of attraction. The state of the system can be measured at intervals of time τ. We define probabilities $P(i_1, i_2, \ldots, i_d)$ to be joint probabilities that $X(t = \tau)$ is in box i_1, $X(t = 2\tau)$ is in box $i_2, \ldots,$ and $X(t = d\tau)$ is in box i_d. The conventional definition for the dimensional spectrum D_q is

$$D_q = \frac{1}{q-1} \lim_{l \to 0} \frac{\ln \sum_{i_1, \ldots, i_d} P^q(i_1, i_2, \ldots, i_d)}{\ln l} \tag{9}$$

Typical chaotic attractors are multifractal (Hentschel and Procaccia, 1983) in that their dimension D_q varies with the index q, where $q \in (-\infty, +\infty)$, thus providing a spectrum of Renyi dimensions. The generalized dimensions are exponents that characterize the nonuniformity of the attractor: positive q's give information on the denser regions of the attractor and negative q's give information on the rarer regions.

The most frequently used dimensions are the Hausdorff (also known as the Kolmogorov capacity) dimension D_0, the information dimension D_1, and the correlation dimension D_2 (Grassberger and Procaccia, 1983*a*,*b*). D_0 and D_1 are obtained in the limits $q \to 0$ and $q \to 1$, respectively. For the total set of generalized dimensions it can be shown (Hentschel and Procaccia, 1983) that $D_q < D_{q'}$ if $q' < q$. Numerical evidence suggests that the Lyapunov dimension D_L is an upper bound on the information dimension D_1.

The function D_q can be obtained from the generalized correlation integral (Pawelzik and Schuster, 1987):

$$C_q^d(l) = \lim_{\substack{l \to 0 \\ N \to \infty}} \left\{ \frac{1}{N} \sum_{i=1}^{N} \left[\frac{1}{N} \sum_{j=1}^{N} \Theta\left(1 - \left[\sum_{n=1}^{d} |X_{i+d} - X_{j+d}|^2 \right]^{1/2} \right) \right]^{q-1} \right\}^{1/(q-1)} \tag{10}$$

where the Heaviside function Θ counts how many pairs of points (X_i, X_j) are situated within a distance l. The spectrum of dimensions is then determined by

$$D_q = \frac{d[\log C_q^d(l)]}{d[\log l]}$$

as obtained over a sufficiently linear scaling range. By far the easiest dimension to compute is the correlation dimension D_2. In order to clarify the application of the correlation integral, we obtain the correlation dimension for the Hénon mapping of equation (2). In Figure 11 we plot a graph of $\log C_2^d(l)$ vs. $\log l$, from which the correlation dimension D_2 can be obtained. The time series consisted of 12,000 consecutive iterations of the map for the parameters $a = 1.4$ and $b = 0.3$ corresponding to the strange attractor of Figure 2a. For increasing embedding dimension d the slope of the linear region in Figure 11 converges to $D_2 = 1.22 \pm 0.02$, in agreement with Grassberger and Procaccia (1983*c*). Similar calculations have given the values of D_2 for the Lorenz and Mackey-Glass systems and these are tabulated in Table I. In all cases the Lyapunov dimension D_L is an upper bound on the correlation dimension D_2.

One of the most important measures by which chaotic motion in spaces of arbitrary dimension can be characterized is the Kolmogorov entropy (Kolmogorov, 1959). It measures the average rate at which information about the state of a dynamical system is lost with time and is defined by analogy to the information entropy of Shannon (Shannon and Weaver,

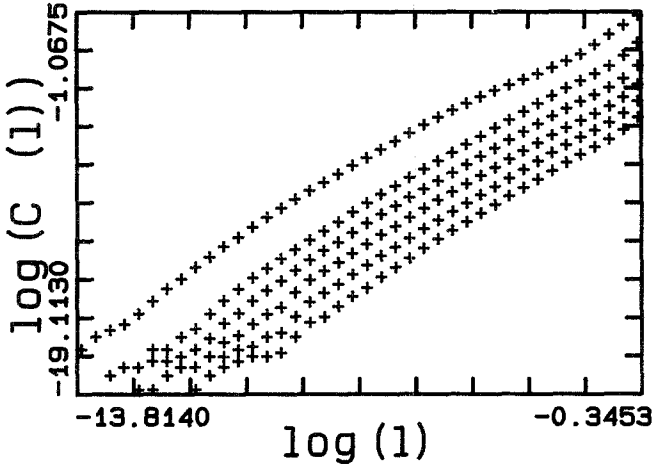

Fig. 11. Correlation integral $\log C_2^d(l)$ vs. $\log l$ for the Hénon map with parameter values $a = 0.3$ and $b = 1.4$. The different results are for different embedding dimensions, namely $d = 2$ (top curve), 4, 6, 8, and 12 (bottom curve).

1949; Schuster, 1988):

$$K = -\lim_{\tau\to 0}\lim_{l\to 0}\lim_{d\to\infty}\frac{1}{\tau d}\sum_{i_1\ldots i_d} P(i_1,\ldots,i_d)\log P(i_1,\ldots,i_d)$$

K is zero for regular motion, it is infinite in random systems, and it is a constant larger than zero if the system displays deterministic chaos. It is inversely proportional to the time interval over which the state of a chaotic system can be predicted. For one-dimensional maps, K is just the (positive) LCE. In higher-dimensional systems, K is the sum of the positive LCE's (Pesin, 1977). Just as we generalized the concept of dimension, we can also define a generalized K entropy (Schuster, 1988),

$$K_q = -\lim_{l\to 0}\lim_{d\to\infty}\frac{1}{d}\frac{1}{q-1}\ln\sum_{i_1\ldots i_d} P^q(i_1,\ldots,i_d)$$

The universal properties of strange point sets can be powerfully catalogued by the Legendre transform $f(\alpha)$ of the D_q (Halsey *et al.*, 1986):

$$\alpha(q) = \frac{d}{dq}[(1-q)D_q] \tag{11a}$$

$$f(\alpha) = q\alpha(q) - (q-1)D_q \tag{11b}$$

Using the qth-order correlation integral equation (9), we can calculate D_q and therefore the $f(\alpha)$ spectrum. The universal function $f(\alpha)$ characterizes the static distribution of points on the attractor with singularities of strength α. In Figure 12 we show the probability distribution of points on the Hénon attractor of Figure 2a. The full complexity of the scaling structure at the onset of chaos (Halsey *et al.*, 1986) through to fully developed turbulence (Chhabra *et al.*, 1989; Meneveau *et al.*, 1990) is contained within the continuous spectrum of exponents α and their densities $f(\alpha)$. These scaling functions are easier to use than the scaling functions introduced by Feigenbaum (1978, 1979) to describe the onset of chaos, which are nowhere differentiable and hence are very difficult to use. These considerations and in particular the global universality of the $f(\alpha)$ spectrum have made the determination of $f(\alpha)$ spectra for physical systems (both theoretical and experimental) a major industry.

The function $f(\alpha)$ has the following universal properties:

$$\frac{df}{d\alpha} = q \quad \text{and} \quad \frac{d^2f}{d\alpha^2} < 0 \tag{12}$$

from which it follows that $D_0 = f_{\max}$, $D_{-\infty} = \alpha_{\max}$, and $D_{+\infty} = \alpha_{\min}$. Thus, for any attractor the curve $f(\alpha)$ will be convex with a single maximum at $q = 0$ and with infinite slopes at $q = \pm\infty$.

All the above functions are related. Both the generalized dimension D_q and entropy K_q can be obtained from the generalized correlation integral.

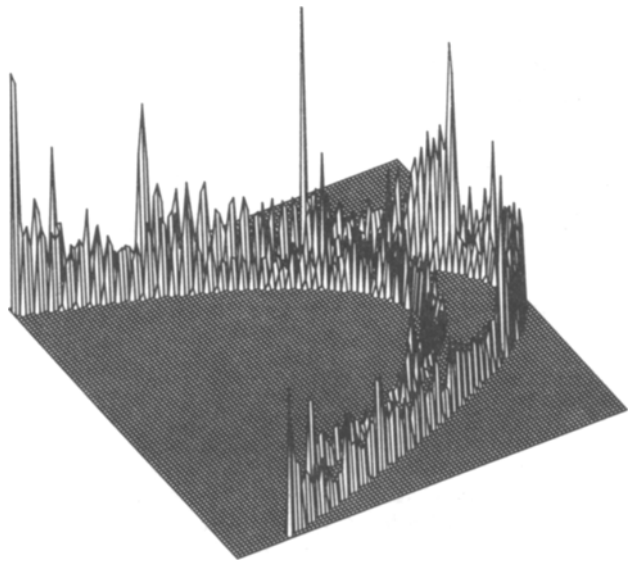

Fig. 12. The probability distribution of points on the Hénon attractor of Figure 2a.

It can be shown that (Schuster, 1988)

$$\lim_{l\to 0}\lim_{d\to\infty}\log C_q^d(l) = (q-1)D_q \ln l + d(q-1)K_q$$

Hence, given a time series generated from computer simulation or from an experiment, a plot of $\log C_q^d$ vs. $\log l$ for fixed q and different values of d, will give us D_q from the slope of the lines and in the limit of large d these lines will converge on the y axis to give K_q. From the Legendre transform of D_q we can then obtain $f(\alpha)$. In theory, then, given experimental or computer-generated data, a reasonable characterization of chaos within a system can be achieved. In practice, noise and insufficient data sets, among other things, make this a difficult task.

8. CONCLUSION

We have given a brief introduction to the field of study known as chaos. To illustrate the fundamental ideas involved, we reviewed three classic systems displaying chaos, namely, the Hénon, Lorenz, and Mackey-Glass systems. Concepts necessary to characterize chaos, such as dimension, $f(\alpha)$ spectra, and entropy, were reviewed. The characterization of chaos is fundamental to physics and this brief introduction we hope will serve to bring scientists and engineers in touch with recent developments.

ACKNOWLEDGMENTS

This work was supported by EOLAS, the Irish National Board for Science and Technology.

REFERENCES

Bergé, P., Pomeau, Y., and Vidal, V. (1987). *Order Within Chaos*, Wiley, New York.
Chhabra, A., Meneveau, C., Jensen, R., and Sreenivasan, K. (1989). *Physical Review A*, **40**, 5284.
Crutchfield, J., Farmer, J., Packard, N., and Shaw, R. (1986). *Scientific American*, **225**(6), 38.
Cvitanovic, P. (1989). *Universality in Chaos*, Adam Hilger, Bristol, England.
De Oliveira, C., and Malta, C. (1987). *Physical Review A*, **36**, 3997.
Duhem, P. (1906). *La Théorie Physique. Son Objet et sa Structure*, Chevalier et Rivière, Paris.
Eckmann, J., and Ruelle, D. (1985). *Review of Modern Physics*, **57**, 617.
Farmer, D. (1982). *Physics*, **4D**, 366.
Feigenbaum, M. (1978). *Journal of Statistical Physics*, **19**, 25.
Feigenbaum, M. (1979). *Journal of Statistical Physics*, **21**, 669.
Grassberger, P., and Procaccia, I. (1983*a*). *Physical Review Letters*, **50**, 346.
Grassberger, P., and Procaccia, I. (1983*b*). *Physical Review A*, **29**, 2591.
Grassberger, P., and Procaccia, I. (1983*c*). *Physica D*, **9**, 189.
Hadamard, J. (1898). *Journal de Mathematiques Pures et Appliquées*, **4**, 27.
Haken, H. (1978). *Synergetics*, Springer, Berlin.
Halsey, T., Jensen, M., Kadanoff, L., Procaccia, I., and Shraiman, B. (1986). *Physical Review A*, **33**, 1141.
Hao, Bai-lin (1984). *Chaos*, World Scientific, Singapore.
Hénon, M. (1976). *Communications in Mathematical Physics*, **50**, 69.
Hentschel, H., and Procaccia, I. (1983). *Physica D*, **8**, 435.
Hirsch, M., and Smale, S. (1965). *Differential Equations, Dynamic Systems and Linear Algebra*, Academic Press, New York.
Hopf, F., Kaplan, M., Rose, M., and Saunders, L. (1986). *Physical Review Letters*, **57**, 1394.
Kaplan, J., and Yorke, J. (1979). *Chaotic Behaviour of Multidimensional Difference Equations*, Springer, Berlin.
Kolmogorov, A. (1959). *Doklady Akademii Nauk SSSR*, **98**, 527.
Lorenz, E. (1963). *Journal of Atmospheric Science*, **20**, 130.
Mackey, M., and Glass, L. (1977). *Science*, **197**, 287.
Marsden, J., and McCracken, M. (1976). *The Hopf Bifurcation and its Applications*, Springer-Verlag, Berlin.
Meneveau, C., Sreenivasan, K., Kailasnath, P., and Fan, M. (1990). *Physical Review A*, **41**, 894.
Pawelzik, K., and Schuster, H. (1987). *Physical Review A*, **35**, 481.
Pesin, Ya. B. (1977). *Mathematical Surveys*, **32**(4), 55.
Poincaré, H. (1908). *Science et Méthode*, Ernest Flammarion, Paris.
Ruelle, D. (1990). *Proceedings of the Royal Society of London A*, **427**, 241.
Ruelle, D., and Takens, F. (1971). *Mathematical Physics*, **20**, 167.
Schuster, H. (1988). *Deterministic Chaos*, 2nd ed., VCH, Weinheim.
Shannon, C., and Weaver, W. (1949). *The Mathematical Theory of Information*, University of Illinois Press, Urbana, Illinois.
Smale, S. (1967). *Bulletin of the American Mathematical Society*, **73**, 474.
Vallée, R., and Delisle, C. (1974). *Physical Review A*, **34**, 309.
Wilson, K., and Kogut, J. (1974). *Physics Report*, **12C**, 75.